

A Metropolis-Adjusted Langevin Algorithm for Sampling Jeffreys Prior

Yibo Shi, Braghadeesh Lakshminarayanan and Cristian R. Rojas

Abstract—Inference and estimation are fundamental aspects of statistics, system identification and machine learning. For most inference problems, prior knowledge is available on the system to be modeled, and Bayesian analysis is a natural framework to impose such prior information in the form of a prior distribution. However, in many situations, coming out with a fully specified prior distribution is not easy, as prior knowledge might be too vague, so practitioners prefer to use a prior distribution that is as ‘ignorant’ or ‘uninformative’ as possible, in the sense of not imposing subjective beliefs, while still supporting reliable statistical analysis. Jeffreys prior is an appealing uninformative prior because it offers two important benefits: (i) it is invariant under any re-parameterization of the model, (ii) it encodes the intrinsic geometric structure of the parameter space through the Fisher information matrix, which in turn enhances the diversity of parameter samples. Despite these benefits, drawing samples from Jeffreys prior is a challenging task. In this paper, we propose a general sampling scheme using the Metropolis-Adjusted Langevin Algorithm that enables sampling of parameter values from Jeffreys prior, and provide numerical illustrations of our approach through several examples.

I. INTRODUCTION

Mathematical models are essential tools for analyzing, predicting, and controlling complex physical processes. System identification is a discipline that deals with the construction of such models from experimental input-output data [1], [2]. A central task within system identification is parameter estimation: given a chosen (or presumed) model structure, the goal is to infer its unknown parameters from observed data. Classical approaches include Prediction Error Methods [1], Instrumental Variables [3], Subspace Methods [4], and Maximum Likelihood Estimation [5]. These methods typically yield point estimates that are often consistent and sometimes asymptotically efficient. Nonetheless, because the dataset used for estimation is inherently finite, there remains a level of uncertainty in the resulting parameter estimates that must be addressed. To rigorously capture and incorporate this uncertainty, Bayesian parameter estimation provides a systematic probabilistic framework, enhancing inference reliability and robustness.

In the Bayesian framework [6], parameter estimation is updated via Bayes’ theorem when observational data become available, producing a posterior distribution that reflects the newly inferred probabilities of the model parameters.

This work has been partially supported by the Swedish Research Council under contract numbers 2016-06079 (NewLEADS) and 2023-05170, and by the Wallenberg AI, Autonomous Systems and Software Program (WASP) funded by the Knut and Alice Wallenberg Foundation. The authors are with the Division of Decision and Control Systems, KTH Royal Institute of Technology, SE-100 44 Stockholm, Sweden. Emails: {yibos, blak, crro}@kth.se

Mathematically, the posterior’s log-density can be decomposed into: (i) the log-likelihood, which measures how well parameters explain observations, and (ii) the log-prior, which encodes initial beliefs. This formulation reveals that the prior distribution inherently acts as a regularization term [7], [8]. For instance, Laplace priors enforce sparsity via l_1 regularization, while Gaussian priors impose l_2 -type constraints on parameter magnitude. Consequently, the choice of prior directly influences the balance between fitting the data and imposing constraints during posterior inference, shaping the final parameter estimates.

Among all possible prior probability densities, Jeffreys prior [9], [10] offers several advantages: (i) it has minimal subjective influence, making it a suitable default in the absence of strong domain-specific information; (ii) its form remains consistent under invertible transformations of the parameter, thus, in practice, Jeffreys prior ensures that posterior updates remain invariant to arbitrary parameter transformations, avoiding the bias introduced by coordinate choices; and (iii) the prior is proportional to the square root of the determinant of the Fisher Information Matrix (FIM), thus it encodes the intrinsic geometric structure of the parameter space. This last property is particularly valuable in data-driven parameter estimation [11], where the induced Riemannian geometry facilitates sampling diverse parameter values. Such diversity enhances the robustness of machine learning models trained on these samples, as the parameters reflect distinct regions. Despite these advantages, Jeffreys prior faces practical limitations. Computing the Fisher information matrix (FIM) in closed form may be intractable or prohibitively expensive for complex or high-dimensional models. While numerical approximations can yield partial FIM estimates, they introduce additional uncertainty in the sampling process: the derived potential function is subject to estimation errors, potentially degrading performance in naive sampling schemes. Furthermore, Jeffreys prior’s normalizing constant is rarely known explicitly, even if the parameter space is bounded and the prior is integrable, complicating direct sampling.

These difficulties are typically addressed through Markov chain Monte Carlo (MCMC) methods, which are widely used for sampling from challenging or high-dimensional distributions [12]. Among these, Langevin-based Monte Carlo (LMC) [13] employs gradient information to guide proposals efficiently in parameter space. Most research on advanced variants addresses some specific challenges of LMC. For instance, Constrained Ensemble LMC [14] ensures physically or statistically valid sample updates by projecting the samples onto constraint sets at each iteration; the Metropolis–

Adjusted Langevin Algorithm (MALA) augments LMC with a Metropolis–Hastings accept/reject step, correcting discretization errors and guaranteeing exact convergence to the target distribution regardless of moderate step-size misspecifications [13], [15]. Among the LMC variants, MALA offers a straightforward way to handle constraints and correct for discretization errors while preserving the geometric advantages of Jeffreys prior via a gradient-based proposal mechanism.

In this paper, we introduce a MALA-based scheme for sampling Jeffreys prior in two distinct scenarios: (i) when the FIM can be derived analytically, and (ii) when an analytical form of the FIM is unavailable, but the score function can be estimated via particle filtering [16], [17], allowing us to compute an approximate FIM that is then used within MALA. Furthermore, we demonstrate an application of Jeffreys prior to generate a diverse set of parameter samples to enhance the performance of a data-driven estimator, by providing improved estimates of the parameters of a model. Our main contributions include:

- A MALA-based sampling approach tailored specifically to Jeffreys prior;
- Extension of this scheme to nonlinear dynamical systems through particle-filter-based FIM estimation;
- Application of sampled Jeffreys prior to promote informative and diverse parameter sets for data-driven estimation methods, thus improving their performance.

The remainder of the paper is organized as follows: in Section II, we define the problem statement. Section III introduces the proposed algorithm to sample from Jeffreys prior based on MALA, while Section IV provides several numerical illustrations of our method. Finally, we conclude the paper in Section V.

II. PROBLEM STATEMENT

Consider a family of probability distributions $\{p(\cdot; \boldsymbol{\theta}) : \boldsymbol{\theta} \in \Theta\}$ defined on a sample space \mathcal{Y} , where $\Theta \subseteq \mathbb{R}^d$ is the parameter space.¹ The FIM at a given parameter value $\boldsymbol{\theta}$, denoted by $\mathbf{J}_{\boldsymbol{\theta}}$, is defined as

$$\mathbf{J}_{\boldsymbol{\theta}} = \mathbb{E}_{y \sim p(\cdot; \boldsymbol{\theta})} \left[\nabla_{\boldsymbol{\theta}} \ln p(y; \boldsymbol{\theta}) \nabla_{\boldsymbol{\theta}^T} \ln p(y; \boldsymbol{\theta}) \right], \quad (1)$$

where $y \in \mathcal{Y}$ denotes the observations, $\nabla_{\boldsymbol{\theta}}$ denotes the gradient with respect to $\boldsymbol{\theta}$, and the expectation operator $\mathbb{E}_{y \sim p(\cdot; \boldsymbol{\theta})}[\cdot]$ is defined as

$$\int_{\mathcal{Y}} [\cdot] p(y; \boldsymbol{\theta}) dy.$$

Intuitively, $\mathbf{J}_{\boldsymbol{\theta}}$ measures the local sensitivity of the log-likelihood to changes in $\boldsymbol{\theta}$ and can be viewed as a Riemannian metric on the parameter space Θ [18].

In practice, computing $\mathbf{J}_{\boldsymbol{\theta}}$ for many complex or high-dimensional models can be analytically intractable or computationally prohibitive, especially when the distributions lack closed-form expressions (see, e.g., [17] for an example

in nonlinear dynamical systems). Consequently, one often resorts to approximate or Monte Carlo methods to estimate $\mathbf{J}_{\boldsymbol{\theta}}$. For instance, given a finite dataset $\{y_i\}_{i=1}^n \subset \mathcal{Y}$, one can compute sample-based estimates $\hat{\mathbf{J}}_{\boldsymbol{\theta}}$ by replacing the expectation in (1) with an empirical average [17].

Jeffreys prior [9] is an uninformative prior distribution on the parameter space Θ . Concretely, Jeffreys prior $\pi(\boldsymbol{\theta})$ is defined (up to a constant factor) by

$$\pi(\boldsymbol{\theta}) \propto \sqrt{\det(\mathbf{J}_{\boldsymbol{\theta}})}, \quad (2)$$

where $\mathbf{J}_{\boldsymbol{\theta}}$ is the FIM defined in (1) and $\det(\cdot)$ denotes the determinant function.

One key advantage of Jeffreys prior over alternative uninformative priors is its reparameterization invariance. If one changes variables from $\boldsymbol{\theta}$ to $\boldsymbol{\phi} = g(\boldsymbol{\theta})$ via a smooth invertible transformation, the associated Jeffreys prior adjusts automatically, preserving the same degree of “non-informativeness” in the new parameter space. This property makes Jeffreys prior a canonical choice when one wishes to impose as little subjective structure as possible.

Most importantly, Jeffreys prior’s explicit dependence on the FIM $\mathbf{J}_{\boldsymbol{\theta}}$ has a Riemannian geometric interpretation. Indeed, as mentioned above, a suitable Riemannian metric on Θ is given by the FIM $\mathbf{J}_{\boldsymbol{\theta}}$. In particular, $\Delta \boldsymbol{\theta}^T \mathbf{J}(\boldsymbol{\theta}) \Delta \boldsymbol{\theta}$ is a good measure of how “different” the probability distributions $p(\cdot; \boldsymbol{\theta})$ and $p(\cdot; \boldsymbol{\theta} + \Delta \boldsymbol{\theta})$ are, for $\Delta \boldsymbol{\theta}$ sufficiently small [19]. Since such a metric induces a natural volume element of the form $d\text{vol} = \sqrt{\det(\mathbf{J}_{\boldsymbol{\theta}})} d\theta^1 \wedge \dots \wedge d\theta^d$ [18, pp. 233], it helps us to distribute samples from Θ according to this volume element so that these samples are well distributed in the parameter space.

Sampling from Jeffreys prior is thus highly relevant in system identification, machine learning, and statistics, but poses two main challenges (i) for complex models, computing or approximating the FIM can introduce uncertainty, and (ii) the normalizing constant of Jeffreys prior is rarely known, complicating direct sampling. The objective of this paper is to address these challenges by proposing an LMC approach that generates Markovian samples whose stationary distribution corresponds precisely to Jeffreys prior $\pi(\boldsymbol{\theta})$.

III. PROPOSED METHOD

In this section, we present the MALA-based method for sampling from Jeffreys prior. The proposed approach accommodates two scenarios: one where the FIM can be computed analytically, and the other where it must be approximated. By unifying these cases under the MALA framework, we enable sampling from the Jeffreys prior across a broad class of parameterized systems, regardless of whether the FIM has a closed-form or is numerically derived.

A. Langevin-based Monte Carlo

The LMC provides an efficient, gradient-based framework for exploring the Jeffreys prior distribution. In this setting, we generate samples distributed according to

$$\boldsymbol{\theta} \sim \pi(\boldsymbol{\theta}) \propto \exp(-V(\boldsymbol{\theta})) \quad (3)$$

¹Throughout this paper, we use boldface fonts (e.g., $\boldsymbol{\theta}$) to refer to vector or matrix variables and normal fonts (e.g., θ) for scalar variables.

by simulating the following Langevin stochastic differential equation (SDE) [20]:

$$d\boldsymbol{\theta}_t = -\nabla_{\boldsymbol{\theta}} V(\boldsymbol{\theta}_t) dt + \sqrt{2} d\mathbf{w}_t, \quad (4)$$

where \mathbf{w}_t denotes standard Brownian motion in \mathbb{R}^d , and $V: \mathbb{R}^d \rightarrow \mathbb{R}$ is a differentiable potential function.

A standard numerical method to simulate (4) numerically is the Euler–Maruyama method [21]. Discretizing time in steps of size τ , we obtain

$$\boldsymbol{\theta}_{i+1} = \boldsymbol{\theta}_i - \tau \nabla_{\boldsymbol{\theta}} V(\boldsymbol{\theta}_i) + \sqrt{2\tau} (\mathbf{w}_{i+1} - \mathbf{w}_i), \quad (5)$$

$$= \boldsymbol{\theta}_i - \tau \nabla_{\boldsymbol{\theta}} V(\boldsymbol{\theta}_i) + \sqrt{2\tau} \boldsymbol{\xi}_i, \quad (6)$$

where $\boldsymbol{\xi}_i \sim \mathcal{N}(\mathbf{0}_d, \mathbf{I}_d)$. The discretization step size τ can be fixed or adapted during simulation.

To verify that the SDE in (4) samples from the Jeffreys prior defined in (3), we use the corresponding Fokker–Planck equation [20]. For simplicity, we first consider the one-dimensional case with parameter θ . The Fokker–Planck equation associated with the Langevin SDE

$$d\theta_t = -\frac{dV(\theta_t)}{d\theta} dt + \sqrt{2} d\mathbf{w}_t$$

describes the time evolution of the probability density $p(\theta, t)$ according to [20]

$$\frac{\partial p(\theta, t)}{\partial t} = -\frac{\partial}{\partial \theta} \left[p(\theta, t) \frac{dV(\theta)}{d\theta} \right] + \frac{\partial^2 p(\theta, t)}{\partial \theta^2}.$$

In the steady-state regime $\partial p(\theta, t)/\partial t = 0$, the probability density reaches a stationary distribution denoted by $p_{\infty}(\theta)$. Imposing zero probability flux at the boundaries (or as $|\theta| \rightarrow \infty$), we obtain

$$p_{\infty}(\theta) \propto \exp(-V(\theta)).$$

Hence, the normalized stationary distribution is

$$p_{\infty}(\theta) = \frac{\exp(-V(\theta))}{Z},$$

where $Z \in \mathbb{R}^+$ is a normalizing constant.

If we specifically define the potential function as

$$V(\theta) = -\frac{1}{2} \ln \det(\mathbf{J}_{\theta}), \quad (7)$$

then it follows from (III-A) that

$$p_{\infty}(\theta) = \frac{1}{Z} \sqrt{\det(\mathbf{J}_{\theta})} \propto \pi(\theta).$$

Thus, the stationary distribution associated with the Langevin SDE (4) exactly coincides with Jeffreys prior. This result is a classical consequence of the relationship between the Fokker–Planck equation and its associated Itô diffusion [22], which underlies the theoretical foundations of LMC methods [13], [23].

Using the update rule in (6) directly to sample from $\pi(\boldsymbol{\theta})$ is referred to as Unadjusted Langevin Algorithm (ULA). It performs an iteration of (6) to generate the samples $\boldsymbol{\theta}_i$ for $i = 0, 1, 2, \dots$, which approximates the target distribution $\pi(\boldsymbol{\theta})$ after a sufficient burn-in period. However, ULA is highly sensitive to the choice of step size τ . If τ is excessively

large, discretization errors introduce bias into the invariant distribution or even cause divergence; if too small, the chain suffers slow mixing, resulting in computational inefficiency. Moreover, practical applications often require the sampled parameter $\boldsymbol{\theta}_i$ to stay in the constrained parameter space $\Theta_c \subset \Theta$ due to physical limitations or prior knowledge. ULA lacks a mechanism to enforce these constraints, potentially proposing values outside the feasible region. In the following subsection, we describe the MALA framework, which addresses these limitations, providing robust and efficient sampling from Jeffreys prior.

B. Metropolis-Adjusted Langevin Algorithm

MALA improves upon ULA by introducing a Metropolis–Hastings accept/reject step that compensates for the errors induced by the discretization. Note that in (6), the proposed variable $\boldsymbol{\theta}_{t+1}$ follows the Gaussian distribution:

$$\boldsymbol{\theta}_{t+1} \sim \mathcal{N}(\boldsymbol{\theta}_t - \tau \nabla_{\boldsymbol{\theta}} V(\boldsymbol{\theta}_t), 2\tau). \quad (8)$$

The proposal density can thus be explicitly written as

$$q(\boldsymbol{\theta}_{t+1} | \boldsymbol{\theta}_t) \propto \exp\left(-\frac{\|\boldsymbol{\theta}_{t+1} - \boldsymbol{\theta}_t + \tau \nabla_{\boldsymbol{\theta}} V(\boldsymbol{\theta}_t)\|_2^2}{4\tau}\right). \quad (9)$$

Given a proposed sample $\boldsymbol{\theta}'$, MALA accepts it with probability [15]

$$\rho^{\text{MALA}}(\boldsymbol{\theta}', \boldsymbol{\theta}_t) = \min\left\{1, \frac{\exp(-V(\boldsymbol{\theta}')) q(\boldsymbol{\theta}_t | \boldsymbol{\theta}')}{\exp(-V(\boldsymbol{\theta}_t)) q(\boldsymbol{\theta}' | \boldsymbol{\theta}_t)}\right\}. \quad (10)$$

If the proposal is accepted, the chain advances as $\boldsymbol{\theta}_{t+1} = \boldsymbol{\theta}'$; otherwise, it remains at the current position, $\boldsymbol{\theta}_{t+1} = \boldsymbol{\theta}_t$. This ensures that the chain remains exactly invariant with respect to $\pi(\boldsymbol{\theta})$ under mild conditions, yielding more robust sampling compared to ULA [15]. Furthermore, MALA inherently accommodates constrained parameter spaces $\boldsymbol{\theta} \in \Theta_c$ by modifying the acceptance probability as follows:

$$\rho_c^{\text{MALA}}(\boldsymbol{\theta}', \boldsymbol{\theta}_t) = \begin{cases} \rho^{\text{MALA}}(\boldsymbol{\theta}', \boldsymbol{\theta}_t), & \text{if } \boldsymbol{\theta}' \in \Theta_c, \\ 0, & \text{otherwise.} \end{cases}$$

Therefore, the accept/reject step based on ρ_c^{MALA} automatically discards proposals that violate these bounds, thereby preserving both the feasibility and the accuracy of the sampling process.

C. Sampling with Estimated FIM

For certain systems with an analytical form of the FIM, we can directly define our potential function as the multivariate form as a generalization of (7),

$$V(\boldsymbol{\theta}) = -\frac{1}{2} \ln \det(\mathbf{J}_{\boldsymbol{\theta}}), \quad (11)$$

with its gradient as

$$\nabla_{\boldsymbol{\theta}} V(\boldsymbol{\theta}) = -\frac{1}{2} \text{tr} \left[\mathbf{J}_{\boldsymbol{\theta}}^{-1} \frac{\partial \mathbf{J}_{\boldsymbol{\theta}}}{\partial \boldsymbol{\theta}} \right], \quad (12)$$

to sample from Jeffreys prior via MALA.

In many dynamic systems, particularly nonlinear state-space (NLSS) models, closed-form expressions for FIMs are not available. In such cases, one must resort to numerical approximations. In this paper, we adopt a particle-filter-based approach to estimate the FIM, following [17], whereby Forward Filtering–Backward Smoothing (FFBSm) provides an unbiased Monte Carlo approximation of the score function, and consequently, the FIM. Despite the inherent stochasticity of particle filters, the resulting estimates are consistent and converge to the true FIM under standard regularity conditions as the number of particles increases.

Remark 1. *For a concrete illustration of particle-filter-based FIM estimation within our framework, we refer the reader to the NLSS model simulation in Section IV.*

Given the estimated FIM $\hat{\mathbf{J}}\boldsymbol{\theta}$, the gradient $\partial\mathbf{J}_{\boldsymbol{\theta}}/\partial\boldsymbol{\theta}$ can be approximated by the one-point unbiased estimate. Specifically, we introduce a random perturbation $\boldsymbol{\mu} \sim \mathcal{N}(\mathbf{0}_d, \mathbf{I}_d)$ and approximate the derivative as

$$\frac{\partial\mathbf{J}_{\boldsymbol{\theta}}}{\partial\theta_j} \approx \frac{\mu_j}{\delta} \left(\hat{\mathbf{J}}_{\boldsymbol{\theta}+\delta\boldsymbol{\mu}} - \hat{\mathbf{J}}_{\boldsymbol{\theta}} \right), \quad j = 1, \dots, d, \quad (13)$$

where $\delta > 0$ is a small step size, and $\hat{\mathbf{J}}_{\boldsymbol{\theta}+\delta\boldsymbol{\mu}}$ is computed using the same estimation procedure as for $\hat{\mathbf{J}}_{\boldsymbol{\theta}}$. This estimator is unbiased in expectation (for $\delta \rightarrow 0$) and substantially reduces the computational burden compared to coordinate-wise finite differences.

Remark 2. *Although the use of such an approximate gradient in (13) might introduce errors, the inclusion of a Metropolis–Hastings accept/reject step in our MALA-based scheme compensates for these inaccuracies and ensures that the target distribution $\pi(\boldsymbol{\theta})$ is still preserved [24]. Standard results in MCMC theory (see, e.g., [13], [15]) guarantee that, as long as the gradient estimator is unbiased and its noise is properly accounted for by the acceptance step, the resulting Markov chain will have $\pi(\boldsymbol{\theta})$ as its stationary distribution. This ensures that our methodology accommodates both closed-form and numerically approximated FIMs without sacrificing correctness.*

Algorithm 1 integrates the particle-filter-based FIM estimation with the one-point gradient approximation within MALA. In this way, even when the FIM is only available approximately via particle methods, our approach guarantees convergence to Jeffreys prior. This enables robust sampling for complex nonlinear state-space models, thereby enhancing both prediction and inference in system identification.

IV. NUMERICAL ILLUSTRATIONS

In this section, we present three numerical examples:

- 1) Sanity check: a simple example in which Jeffreys prior can be computed exactly, verifying that Algorithm 1 converges to the correct distribution;
- 2) NLSS system: a sampling example where the FIM is estimated via the particle filter method, showing that Algorithm 1 remains effective with estimated $\mathbf{J}_{\boldsymbol{\theta}}$;
- 3) An application of parameter estimation: a practical setting in which Jeffreys prior sampling outperforms a

Algorithm 1 Sample from Jeffreys Prior Distribution

Require: Initial guess $\boldsymbol{\theta}_0$, possible constrained parameter space Θ_c , step size τ , number of iterations N , small finite-difference parameter $\delta > 0$

- 1: **for** $n = 0, 1, \dots, N - 1$ **do**
- 2: Compute or estimate $\mathbf{J}_{\boldsymbol{\theta}_n}$
- 3: Compute $\nabla_{\boldsymbol{\theta}}V(\boldsymbol{\theta}_n)$ using (12) **or** run
- 4: Draw a random direction $\boldsymbol{\mu} \sim \mathcal{N}(\mathbf{0}_d, \mathbf{I}_d)$
- 5: Estimate $\nabla_{\boldsymbol{\theta}}V(\boldsymbol{\theta})$ using (13)
- 6: Estimate $\mathbf{J}_{\boldsymbol{\theta}+\delta\boldsymbol{\mu}}$
- 7: Compute $\nabla_{\boldsymbol{\theta}}V(\boldsymbol{\theta}_n)$ using (12)
- 8: Sample $\boldsymbol{\xi}_n \sim \mathcal{N}(\mathbf{0}_d, \mathbf{I}_d)$ and $U \sim \mathcal{U}(0, 1)$
- 9: **Propose**

$$\boldsymbol{\theta}' \leftarrow \boldsymbol{\theta}_n - \tau\nabla_{\boldsymbol{\theta}}V(\boldsymbol{\theta}_n) + \sqrt{2\tau}\boldsymbol{\xi}_n,$$

$$\rho_n \leftarrow \begin{cases} \rho^{\text{MALA}}(\boldsymbol{\theta}', \boldsymbol{\theta}_n), & \text{If } \boldsymbol{\theta}' \in \Theta_c, \\ 0, & \text{Otherwise.} \end{cases}$$

- 10: **Accept/reject step**

$$\boldsymbol{\theta}_{n+1} \leftarrow \begin{cases} \boldsymbol{\theta}', & \text{If } U < \rho_n, \\ \boldsymbol{\theta}_n, & \text{Otherwise.} \end{cases}$$

- 11: **end for**

- 12: **return** $\{\boldsymbol{\theta}_n\}_{n=1}^N$
-

uniform prior for synthetic-data generation, improving parameter estimation performance.

We now detail each example in turn.

A. Verification of the Sampling Procedure

1) *Experiment setup:* In this experiment, we apply Algorithm 1 to sample from Jeffreys prior for the Coin-Bending Model introduced in [25]. In this model, the probability $q(\varphi)$ of obtaining heads depends on the bending angle φ according to

$$q(\varphi) = \frac{1}{2} + \frac{1}{2} \left(\frac{\varphi}{\pi} \right)^3.$$

Each coin toss yields a binary outcome random variable Y where

$$Y = \begin{cases} 1, & \text{with probability } \frac{1}{2} + \frac{1}{2} \left(\frac{\varphi}{\pi} \right)^3, \\ 0, & \text{with probability } \frac{1}{2} - \frac{1}{2} \left(\frac{\varphi}{\pi} \right)^3, \end{cases}$$

with 1 denoting heads. Therefore, we can derive the score function in closed form:

$$\nabla_{\varphi} \ln p(Y; \varphi) = \mathbb{1}\{Y = 1\}p_1 - \mathbb{1}\{Y = 0\}p_0,$$

with

$$p_1 = \frac{\frac{3}{\pi} \left(\frac{\varphi}{\pi} \right)^2}{1 + \left(\frac{\varphi}{\pi} \right)^3}, \quad p_0 = \frac{\frac{3}{\pi} \left(\frac{\varphi}{\pi} \right)^2}{1 - \left(\frac{\varphi}{\pi} \right)^3}.$$

The parameter to be estimated is φ . Given n independent coin tosses resulting in observations $\mathbf{y} \in \{0, 1\}^n$, the information J_{φ} per sample can be approximated, if n is sufficiently large, by

$$\hat{J}_{\varphi} = \frac{\mathbf{1}^T \mathbf{y}}{n} p_1^2 + \frac{n - \mathbf{1}^T \mathbf{y}}{n} p_0^2.$$

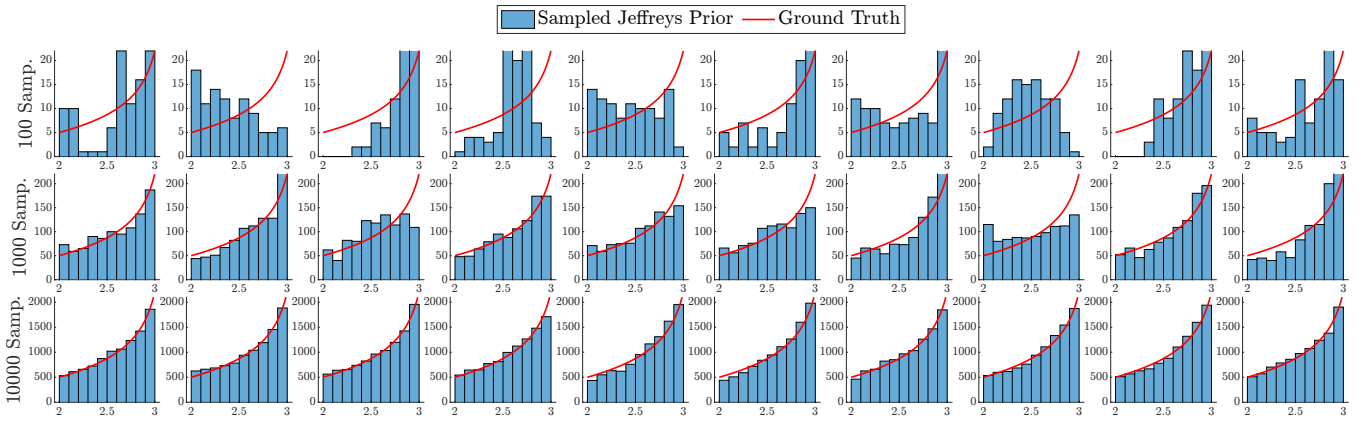


Fig. 1. Histograms of 100 (top), 1000 (middle), and 10000 (bottom) samples of Jeffreys prior and the shape of the true Jeffreys prior (red curve) from the Coin-Bending Model. Each set of sampling experiments contains ten different realizations.

Assuming consistency as $n \rightarrow \infty$, we treat $\pi(\varphi) \propto \sqrt{\hat{J}_\varphi}$ as the ground truth, we define the potential $V(\varphi) = -\frac{1}{2} \ln \hat{J}_\varphi$ with the gradient given explicitly by

$$\nabla V(\varphi) = -\frac{1}{2} \hat{J}_\varphi^{-1} \frac{d\hat{J}_\varphi}{d\varphi}.$$

We run Algorithm 1 to generate samples from $\pi(\varphi)$ within the constrained set $\varphi \in \Phi_c = [2, 3]$. Three experiments are performed with $N = \{100, 1000, 10000\}$ samples, each repeated for 10 independent realizations. The resulting empirical distributions are then compared with the estimated Jeffreys prior to verify convergence and consistency.

2) *Simulation results:* The simulation results are shown in Fig. 1. As illustrated, the empirical distribution of samples obtained by our algorithm gives better match of the theoretical Jeffreys prior as the number of samples increases (from Row 1 to Row 3). Moreover, even with a relatively small sample size (e.g., 1,000 samples), the empirical distribution already closely resembles the exact Jeffreys prior, indicating rapid convergence. Additionally, the difference in the sampled realizations (100 sampled points) reveals the stochastic nature of the chain and demonstrates good mixing behavior, reflecting adequate exploration of the parameter space.

This example provides a clear validation of our proposed MALA-based sampler, as it allows direct comparison between the empirical and exact prior distributions. Furthermore, this one-dimensional scenario enables straightforward assessment of mixing quality and acceptance rates, establishing a solid baseline for applying our approach in more complex, high-dimensional settings.

B. Sampling Jeffreys Prior for a Dynamical System

1) *Experiment setup:* In this example, we demonstrate the performance of Algorithm 1 by sampling from the Jeffreys prior for an NLSS model, where the FIM is numerically approximated using a particle filter. Specifically, we consider the Hull–White stochastic volatility (SV) model [16], [26]

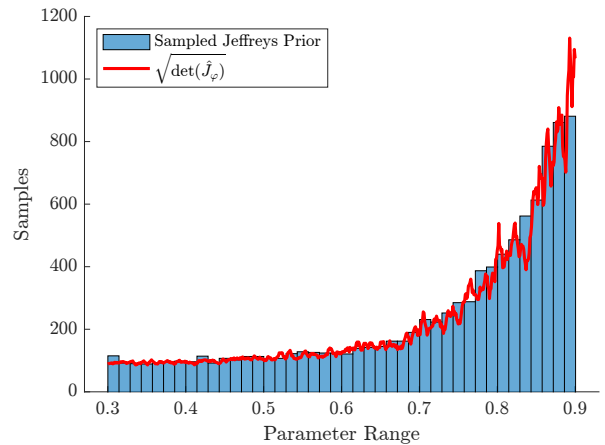


Fig. 2. Histogram of 10000 samples of Jeffreys prior and the shape of the true Jeffreys prior (red curve) from the SV Model.

defined as:

$$\begin{aligned} x_{t+1} | x_t &\sim \mathcal{N}(\varphi x_t + \rho u_t, \sigma_v^2), \\ y_t | x_t &\sim \mathcal{N}(0, \beta^2 \exp(x_t)), \end{aligned}$$

where the control input u_t is generated by samples from a standard normal distribution. Our goal is to sample the Jeffreys prior $\pi(\varphi)$ for the system parameter φ corresponding to the system dynamics, constrained to the feasible region $\Phi_c = [0.3, 0.9]$, ensuring system stability. For simulation, the rest of model parameters are set as

$$[\rho, \sigma_v, \beta] = [0.2, 0.5, 0.7],$$

and the system is simulated for $T = 1000$ time steps.

Since the Fisher information $J(\varphi)$ lacks an analytical form for this model, we estimate it using a particle-filter-based method from [17], as described in Section III, employing $N_p = 1000$ particles and averaging multiple Monte Carlo runs to obtain a reliable estimation $\hat{J}(\varphi)$. Accordingly, we compute the estimated shape of Jeffreys prior $\pi(\varphi) \propto \sqrt{\hat{J}_\varphi}$ and compare it with the distribution of the generated samples.

We define the corresponding potential function as $V(\varphi) = -\frac{1}{2} \ln \hat{J}(\varphi)$ and approximate its gradient $\widehat{\nabla}V(\varphi)$ using (12) and the one-point finite-difference estimator in (13).

Finally, Algorithm 1 is run for $N = 10000$ iterations with step size $\tau = 0.05$, and the generated samples are compared against the estimated shape of Jeffreys prior.

2) *Simulation results:* The histogram of the $N = 10000$ generated samples is shown in Fig. 2, overlaid with the estimated shape of Jeffreys prior $\pi(\varphi) \propto \sqrt{\hat{J}_\varphi}$ computed from the particle filter estimation.

As expected, the estimated Jeffreys prior assigns higher probability near the boundary $\varphi \approx 0.9$, indicating greater parameter sensitivity, and lower probability near the boundary ($\varphi \approx 0.3$).

At the lower boundary $\varphi = 0.3$, the influence of x_t on the evolution of the state is relatively small; the dynamics are then dominated by the input u_t and the process noise v_t , making the likelihood less sensitive to changes in φ . In contrast, around $\varphi = 0.9$, a small perturbation in φ produces significant changes in the predicted states and, hence, in the likelihood function. This leads to a higher Fisher information in that region. Thus, the estimated prior shape confirms that the particle-filter-based FIM estimation is consistent with theoretical expectations.

Moreover, the close agreement observed in Fig. 2 between the histogram of generated samples and the estimated Jeffreys prior verifies that our proposed algorithm reliably samples from the Jeffreys prior even when the FIM is numerically approximated.

Overall, these results demonstrate the validity of our sampling framework and highlight the advantage of leveraging the geometry encoded by the Jeffreys prior for parameter inference and experimental design.

C. An Application of Jeffreys Prior to Parameter Estimation

1) *Experiment setup:* In this example, we illustrate the advantages of sampling from Jeffreys' prior within the Two-Stage (TS) estimation framework, using parameter estimation for a Weibull distribution as a test case. TS provides an effective validation scenario, although the framework itself is well-established. In TS, given a parametric model $p(\cdot; \theta)$ with parameters $\theta \in \Theta \subseteq \mathbb{R}^d$, one constructs a synthetic training dataset of parameter-data pairs

$$\{(\theta_i, \mathbf{y}_i)\}_{i=1}^{M_\theta},$$

where data samples \mathbf{y}_i are generated from $p(\cdot; \theta_i)$. A supervised learning method then builds an estimator:

$$\hat{\theta}(\mathbf{y}) = \mathbf{g}(\mathbf{h}(\mathbf{y})),$$

with a fixed compression function \mathbf{h} and a regression-based function \mathbf{g} . For additional details on the implementation setup of TS, we refer the reader to [27].

In the context of TS, the distribution of the synthetic parameter samples is crucial. We advocate sampling θ according to Jeffreys prior, $\pi(\theta)$ naturally reflects the local identifiability structure of the model. In contrast, a uniform

prior may not account for how informative different regions of the parameter space are, potentially leading to suboptimal training datasets.

The advantage of our approach is that, by sampling the synthetic θ_i values from Jeffreys prior using our proposed algorithm, the resulting training dataset better represents regions where the data is most informative about the parameters.

For the numerical example, we consider the Weibull distribution, widely used in reliability engineering, whose probability density function is given by

$$f(A; \eta, \gamma) = \frac{\gamma}{\eta} \left(\frac{A}{\eta}\right)^{\gamma-1} \exp\left[-\left(\frac{A}{\eta}\right)^\gamma\right], \quad A \geq 0,$$

where $\eta > 0$ is the scale parameter and $\gamma > 0$ is the shape parameter. Thus, the parameter vector is $\theta = [\eta, \gamma]^T$.

2) *Simulation results:* We validate the TS estimators trained under uniform and Jeffreys priors using a validation set consisting of 1000 parameter points $\theta_\ell = [\eta_\ell, \gamma_\ell]^T$ uniformly sampled from $[1, 20] \times [1, 20]$. For each θ_ℓ synthetic data $\{y_\ell^i\}_{i=1}^M$ generated from the Weibull model. We evaluate two classes of TS estimators based on the samples from the uniform and Jeffreys priors respectively.

Fig. 3(a) shows the sampled Jeffreys prior distribution in the (γ, η) parameter space. Notably, Jeffreys prior emphasizes lower values of γ while remaining relatively uniform along η , aligning well with the Weibull model's FIM structure, which indicates higher sensitivity (information content) at smaller γ .

Estimation performances for η and γ are compared in Figs. 3(b) and 3(c), respectively. In Fig. 3(b), both uniform and Jeffreys-based estimators produce accurate and similar results of the scale parameter across its entire range, because Jeffreys prior is nearly uniform in η and thus provides coverage comparable to the uniform prior.

However, notable differences arise for the shape parameter γ , as seen in Fig. 3(c). Near low values of $\gamma < 5$, the uniform-based estimator exhibits significant variance and bias. In contrast, the Jeffreys-based estimator demonstrates considerably improved accuracy and precision in this region, owing to the fact that Jeffreys prior focuses sampling efforts where the Fisher information is greatest. Remarkably, despite allocating fewer training samples to higher γ regions, the Jeffreys-based estimator maintains effective generalization in those regions, underscoring the advantage of information-driven weighting in the parameter space.

Overall, these experiments demonstrate that sampling according to Jeffreys prior within the TS framework substantially enhances estimation accuracy and robustness for shape-dominated parameters, while maintaining comparable performance to the uniform-based estimator along directions of weaker sensitivity. Therefore, the application of Jeffreys prior not only leads to better TS estimators for the Weibull distribution but also suggests that our approach may have broader applicability in synthetic data generation and parameter estimation for complex models.

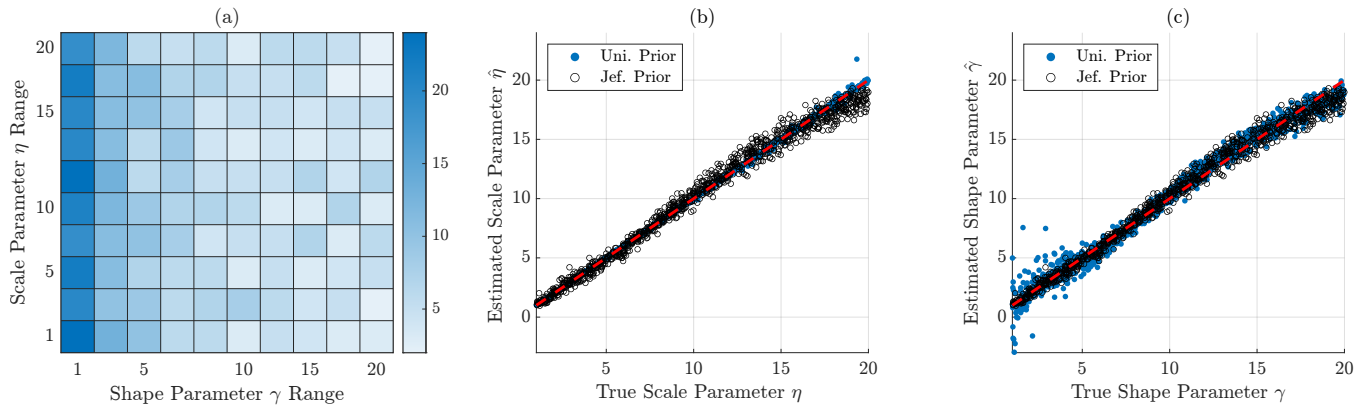


Fig. 3. (a) Heatmap of 1000 samples from Jeffreys prior distribution of the scale (η) and shape (γ) parameters from the Weibull distribution model; (b) Scatter plot of estimated scale parameter $\hat{\eta}$ based on the uniform prior and Jeffreys prior vs. its true value; (c) Scatter plot of estimated shape parameter $\hat{\gamma}$ based on the uniform prior and Jeffreys prior vs. its true value. The red dashed line corresponds to an oracle estimate, which knows the true value of the parameter.

V. CONCLUSIONS

In this paper, we have proposed a MALA-based sampling scheme designed to generate samples from Jeffreys prior. Our approach involves imposing Jeffreys prior as the stationary distribution of a Langevin-based MCMC, where each update step of the Markov chain is determined by the gradient of the logarithm of the determinant of the Fisher Information matrix. Furthermore, for the case when this matrix cannot be computed analytically, we have employed a particle filter algorithm to approximate the score function, thereby estimating the gradient of the log determinant of the FIM. We have validated our sampling scheme through several numerical examples, including one that has demonstrated how the diversity inherent in Jeffreys prior can enhance the estimates produced by a data-driven estimator. In future work, we plan to further explore the use of this sampling scheme for parameter estimation in dynamical systems, particularly using data-driven estimators that require minimal training data, by leveraging the diversity of samples promoted by Jeffreys prior.

REFERENCES

- [1] L. Ljung, *System Identification: Theory for the User, 2nd Ed.* Prentice Hall, 1999.
- [2] T. Söderström and P. Stoica, *System Identification.* Prentice Hall, 1989.
- [3] T. Söderström and P. Stoica, *Instrumental Variable Methods for System Identification.* Springer-Verlag, 1983.
- [4] P. Van Overschee and B. De Moor, *Subspace Identification for Linear Systems: Theory-Implementation-Applications.* Springer, 2012.
- [5] P. E. Caines, “A note on the consistency of maximum likelihood estimates for finite families of stochastic processes,” *The Annals of Statistics*, vol. 3, no. 2, pp. 539–546, 1975.
- [6] J. M. Bernardo and A. F. M. Smith, *Bayesian Theory.* John Wiley & Sons, 2009.
- [7] G. Pillonetto, T. Chen, A. Chiuso, G. De Nicolao, and L. Ljung, *Regularized System Identification: Learning Dynamic Models from Data.* Springer, 2022.
- [8] M. A. T. Figueiredo, “Adaptive sparseness for supervised learning,” *IEEE Transactions on Pattern Analysis and Machine Intelligence*, vol. 25, no. 9, pp. 1150–1159, 2003.
- [9] H. Jeffreys, “An invariant form for the prior probability in estimation problems,” *Proceedings of the Royal Society of London. Series A. Mathematical and Physical Sciences*, vol. 186, no. 1007, pp. 453–461, 1946.
- [10] H. Jeffreys, *The Theory of Probability, 3rd Ed.* Oxford University Press, 1998.
- [11] S. Garatti and S. Bittanti, “A new paradigm for parameter estimation in system modeling,” *International Journal of Adaptive Control and Signal Processing*, vol. 27, no. 8, pp. 667–687, 2013.
- [12] C. P. Robert, G. Casella, and G. Casella, *Monte Carlo statistical methods*, vol. 2. Springer, 1999.
- [13] G. O. Roberts and R. L. Tweedie, “Exponential convergence of Langevin distributions and their discrete approximations,” *Bernoulli*, vol. 2, no. 3, pp. 341–363, 1996.
- [14] Z. Ding and Q. Li, “Constrained Ensemble Langevin Monte Carlo,” *Foundations of Data Science*, vol. 4, no. 1, pp. 37–70, 2022.
- [15] G. O. Roberts and O. Stramer, “Langevin diffusions and metropolis-hastings algorithms,” *Methodology and Computing in Applied Probability*, vol. 4, pp. 337–357, 2002.
- [16] J. Dahlin and F. Lindsten, “Particle filter-based Gaussian process optimisation for parameter inference,” *IFAC Proceedings Volumes*, vol. 47, no. 3, pp. 8675–8680, 2014.
- [17] P. E. Valenzuela, J. Dahlin, C. R. Rojas, and T. B. Schön, “On robust input design for nonlinear dynamical models,” *Automatica*, vol. 77, pp. 268–278, 2017.
- [18] W. M. Boothby, *An Introduction to Differentiable Manifolds and Riemannian Geometry, Revised 2nd Ed.* Academic Press, 2003.
- [19] S. Amari, *Information Geometry and its Applications.* Springer, 2016.
- [20] I. Karatzas and S. E. Shreve, *Brownian Motion and Stochastic Calculus, 2nd Ed.* Springer-Verlag, 1991.
- [21] D. Higham and P. E. Kloeden, *An Introduction to the Numerical Simulation of Stochastic Differential Equations.* SIAM, 2021.
- [22] K. Itô and H. P. McKean, *Diffusion Processes and their Sample Paths.* Springer, 2012.
- [23] A. Gelman, W. R. Gilks, and G. O. Roberts, “Weak convergence and optimal scaling of random walk Metropolis algorithms,” *The Annals of Applied Probability*, vol. 7, no. 1, pp. 110–120, 1997.
- [24] C. Andrieu and G. O. Roberts, “The pseudo-marginal approach for efficient Monte Carlo computations,” *The Annals of Statistics*, vol. 37, no. 2, pp. 697–725, 2009.
- [25] A. Ly, M. Marsman, J. Verhagen, R. P. P. P. Grasman, and E.-J. Wagenmakers, “A tutorial on Fisher information,” *Journal of Mathematical Psychology*, vol. 80, pp. 40–55, 2017.
- [26] J. Hull and A. White, “The pricing of options on assets with stochastic volatilities,” *The Journal of Finance*, vol. 42, no. 2, pp. 281–300, 1987.
- [27] B. Lakshminarayanan and C. R. Rojas, “A statistical decision-theoretical perspective on the two-stage approach to parameter estimation,” in *Proceedings of the 61st IEEE Conference on Decision and Control (CDC)*, pp. 5369–5374, 2022.